

Fluorescent glass embedded silver nanoclusters: An optical study

B. Karthikeyan^{a)}

Light and Matter Physics Group, Raman Research Institute, CV Raman Avenue, Sadashivanagar, Bangalore 560 080, India

(Received 11 December 2007; accepted 26 March 2008; published online 12 June 2008)

In this report, the light emitting behavior of silver nanoclusters embedded in sodalime glass through ion-exchange technique is studied. The cluster sizes were varied through thermal annealing. The optical absorption spectra were recorded for all the glasses. The variation of surface plasmon resonance peak with the annealing temperature was found. Fourier transform infrared spectral measurement was utilized to identify the chemical interface damping. Photoluminescence measurements were carried out and time resolved photoluminescence was performed to identify the time evolution of emission. © 2008 American Institute of Physics. [DOI: [10.1063/1.2936879](https://doi.org/10.1063/1.2936879)]

I. INTRODUCTION

Developments in nanotechnology and nanoscience needs clear insight of nanomaterials, particularly the noble metal nanoparticles. Incorporation of the metal nanoparticle in solid matrix and growth of nanoparticles through different techniques¹ are quite interesting. Usually, the clusters are not very stable in the colloid form but in solid matrix they will stay for longer. There are several reports and interesting results on the nanocomposite glasses, which are prepared through ion-exchange, sol-gel method, and ion implantation techniques.^{2,3} Mie⁴ gave a clear insight regarding the optical properties of metal nanoclusters, not only the size and shape of the metal particles but also the host where the particles are suspended also gain importance through Mie theory. When the particle size is smaller than the skin depth of the metal (for Ag, ~22 nm) and the particle is exposed to the electromagnetic radiation, the interaction of the applied optical electric field will be in the entire volume resulting in dipolar oscillations. However, when the size exceeds this limit, the optical field fails to oscillate the entire free conduction electrons, so that there will be a chance of quadrupolar and higher polar oscillations.

Recently, metallic nanoparticles are gaining much attention due to their fluorescence,^{5,6} enhanced fluorescence of nearby fluorophores⁷ and ions.⁸ Zheng *et al.*⁶ found size selective emission from water soluble Au nanoparticles and their study on Ag₂O (Ref. 9) particles proves that these clusters are potential candidates for optical data storage applications. Similarly, Link *et al.*¹⁰ reported the two distinct emission peaks from the 28 atom Au nanoclusters. Even though there are several reports^{11,12} on silver ion-exchanged glasses about their optical and nonlinear optical properties, in the present report, detailed size-dependent fluorescence emission and time evolution of electron recombination of Ag nanoclusters are studied.

II. EXPERIMENTAL

The metal ions were incorporated into the sodalime glass through the thermal ion-exchange method. The commercial soda lime glasses were cleaned by an ultrasonicator. The glass slides were immersed in the molten salt bath, which has the AgNO₃:NaNO₃ in the 1:3 molar ratio, and the ion-exchange process was done at 350–400 °C for the time period of 1 min. The silver ions in the molten salt bath penetrate and sit in the sites left by the Na⁺ ions, which are the glass modifiers in the host matrix. The prepared glass slides were air annealed at 350, 450, 500, and 550 °C for 1 h and then furnace cooled. Samples were named as Ag-350, Ag-450, Ag-500, and Ag-550, respectively. The annealed samples were found to be different in color due to the various cluster sizes in the surface. Transmission electron micrograph (TEM) of the 550 °C annealed glass was obtained using a Teenai F30 machine. Optical absorption spectra were recorded using a dual beam PerkinElmer optical absorption spectrometer. To identify the local structure, particularly the interaction of Ag clusters with the host matrix, Fourier transform infrared (FTIR) spectroscopy was utilized; the spectra were recorded using a Shimadzu 8000 model spectrometer. Fluorescence spectral measurements were done using a PerkinElmer spectrometer where a Xe lamp was employed as the excitation source. Time resolved fluorescence decays were obtained by the time-correlated single photon counting method. A diode pumped neodymium doped yttrium aluminum garnet continuous wave laser (Millennia, Spectra Physics), with a wavelength of 532 nm, was used to pump the Ti:sapphire (Tsunami, Spectra Physics) laser, which is a femtosecond (100 fs) mode locked laser system. The 840 nm (80 MHz) line was taken from the Ti:sapphire laser and passed through a pulse picker (Spectra Physics, 3980 2S) to generate 4 MHz pulses. The second harmonic output (400 nm, 100 fs) was generated by a flexible harmonic generator (Spectra Physics, GWU 23PS). The vertically polarized 400 nm laser pulses were used to excite the sample. The fluorescence emission at the magic angle (54.78°) was dispersed in a monochromator (*f*/3 aperture), counted by a micro channel plate photomultiplier tube (Hamamatsu R3809), and processed through time to amplitude converter and multichannel

^{a)}Present address: Department of Physics, National Institute of Technology, Tiruchirappalli 605 012. Author to whom correspondence should be addressed. Tel.: +91-0431-2501801. FAX: +91-(0)431-2500133. Electronic mail: balkarin@yahoo.com.

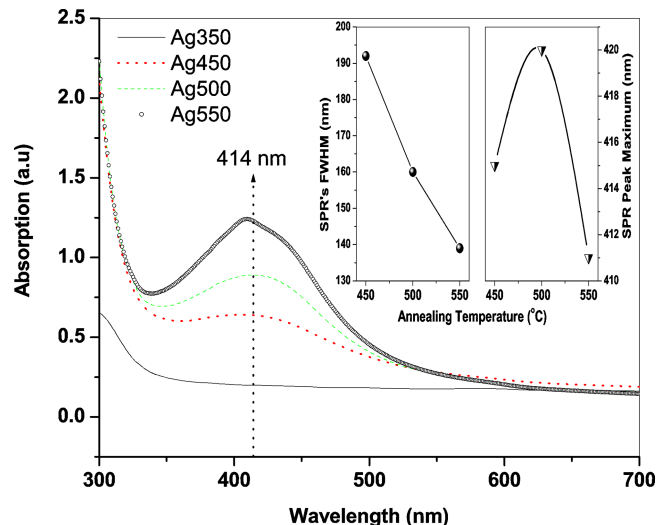


FIG. 1. (Color online) Optical absorption spectra of silver composite glasses that are annealed at different temperatures. The inset shows the variation of SPR peak intensity and SPR's FWHMs with annealing temperature.

analyzer. The instrument response function for this system is ≈ 52 ps. The fluorescence decay was analyzed by using the software provided by IBH(DAS-6) and PTI global analysis software.

III. RESULTS AND DISCUSSION

Figure 1 shows the optical absorption spectra of the prepared glasses, and the surface plasmon resonance (SPR) maximum is found around 415 nm, which is a typical characteristic of Ag nanoclusters. According to the classical Mie theory, the extinction coefficient for small clusters due to SPR is given by⁴

$$\sigma_{\text{ext}}(\omega) = 9V \frac{\omega}{c} \varepsilon_m^{3/2} \frac{\varepsilon_2(\omega)}{[\varepsilon_1(\omega) + 2\varepsilon_m]^2 + \varepsilon_2(\omega)^2}, \quad (1)$$

where V is the particle volume and $\varepsilon_1(\omega) = \varepsilon_1(\omega) + i\varepsilon_2(\omega)$ is the frequency dependent dielectric constant of the nanoparticle. The SPR maximum occurs at that frequency ω_s when $\varepsilon_1(\omega) + 2\varepsilon_m$ becomes zero, where ε_m is the dielectric constant of the host matrix assumed to be real. The SPR peak is size dependent because ω_s is given by $\omega_p / \sqrt{1 + 2\varepsilon_1}$, which is directly proportional to the number of the conduction band electrons n_e through the equation $\omega_p^2 = 4\pi n_e e^2 / m$, where e is the electronic charge, m is the electronic mass, and ω_p is the plasma frequency of the metal.

The broadening of the SPR band is due to chemical interface damping (CID), which is subdivided into two types. The first one is the static charge transfer (SCT),¹³ whereby the electrons in the cluster will tunnel out from the cluster and fill up energy levels of the adsorbate atoms, which are at an equal or lower energy. This reduction of free electrons in the cluster will shift the plasmon oscillation frequency to the red end of the spectrum. For smaller clusters that are smaller than 20 nm, the peak shift in frequency for an electron density change from n_1 to n_2 is given by¹³

$$\Delta\omega_{\text{resonance}} \cong [(n_1)^{1/2} - (n_2)^{1/2}](e^2/\varepsilon_o m_{\text{eff}})^{1/2}(2\varepsilon_m + 1 + \chi_{1,\text{interband}})^{-1/2}, \quad (2)$$

where m_{eff} is the effective mass of the electron and $\chi_{1,\text{interband}}$ is the optical susceptibility for interband transitions.

The second type of CID is known as the dynamic charge transfer (DCT),^{14,15} which plays the role as the host dependence of SPR broadening. In DCT, the cluster-host interface and the chemical properties of the host (which can also be a functional group/adsorbate atom) become important. Here, a temporary charge transfer will occur between the cluster and the surrounding, but the residence time of these electrons will be of the order of a few femtoseconds. The back transferred electrons will undergo inelastic collision/scattering with the electrons in the cluster, which oscillate coherently, thereby broadening the spectrum.

Apart from SCT, cluster's size increase will also show a redshift in the SPR band.¹⁶ In the present case, at higher annealing temperatures, the SPR peak shows a redshift, as shown in the inset of Fig. 1. This normally happens due to the nucleation growth of clusters at higher temperature annealing in solid matrix. In addition to this, the SPR bandwidth [full width at half maximum (FWHM)] decreases with the increase of annealing temperature, which also indicates the size growth of nanoparticles. The SPR bandwidth will depend on the size-dependent parameters A and R (cluster radius) given by¹³

$$\Gamma(A_{\text{size}}, R) \cong \Gamma_o + (2\omega_p^2/\omega^3)v_{\text{Fermi}}[(\partial\varepsilon_1/\partial\omega)^2 + (\partial\varepsilon_2/\partial\omega)^2]^{-1/2}A_{\text{size}}/R, \quad (3)$$

where Γ_o is the SPR bandwidth predicted by Mie's equation. The $1/R$ dependence of Γ is the consequence of two effects: while the number of conduction band electrons participating in the collective excitation is proportional to R^3 , the number of surrounding matrix molecules is only proportional to (R^2) .¹⁴ This is the reason that smaller clusters show higher FWHM than the bigger clusters.

The cluster diameter can be obtained from the FWHM ($\Delta E_{1/2}$) of the SPR band as¹⁷

$$D = hv_F/(\pi\Delta E_{1/2}), \quad (4)$$

where $v_F(1.39 \times 10^8$ cm/s) is the Fermi velocity of electrons in bulk silver and h is Planck's constant. Equation (4) is valid as long as the cluster size is much smaller than the mean free path of the electrons (which is 27 nm in Ag). Using the values of FWHM and SPR peak positions, the diameter of Ag nanoclusters were estimated as 2, 2.7, and 3.3 nm for 450, 500, and 550 °C annealed samples, respectively. This agrees well with our previous study, which is based on low frequency Raman spectral measurements.¹⁸ This results show, as expected, that the diameter of Ag nanoclusters increases with annealing temperature due to the diffusion-limited aggregation.^{19,20} TEM measurement for Ag-550 depicted in Fig. 2 shows that the diameters of the clusters are around 3–4 nm, which agrees well with the above results.

To determine whether CID is taking place in the present case, the FTIR spectra for all the ion-exchanged glasses (shown in Fig. 3) are recorded. There are broad bands at

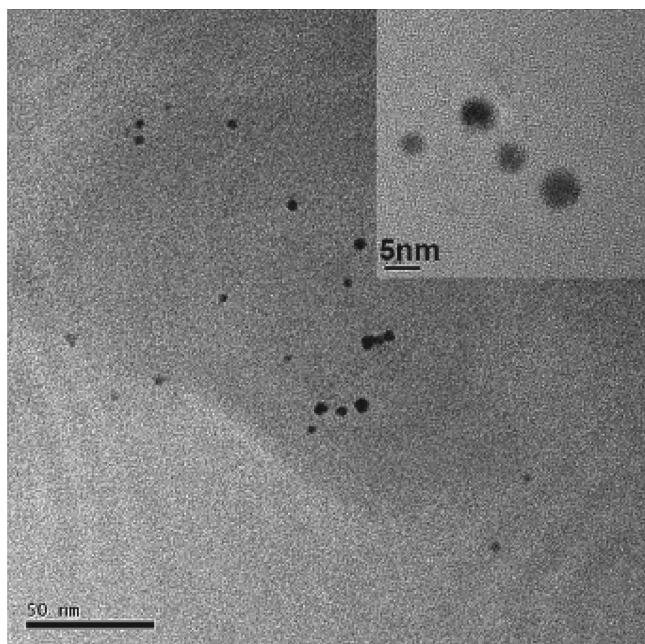


FIG. 2. TEM image of Ag nanoclusters in Ag-550 glass. The inset shows HREM image of the same glass.

1200 and 1044 cm^{-1} , which are typical band absorptions of SiO_4 tetrahedra bridged by oxygen atoms. The band at 773 cm^{-1} is attributed to the symmetric stretching mode of Ag–O–Si bonds, showing that the Ag clusters have oxygen as an adsorbate atom/surrounding atom. There are also some previous reports that confirm the bond between Ag and O.^{21,22} Thus, the bond between Ag and O indirectly supports the assumption of the occurrence of CID in the present clusters.

Figure 4 shows the emission spectra of all the glasses, which are excited at the wavelength of 400 nm (~ 3 eV). From the figure, it is clear that the glass annealed at 350 °C shows intense broad emission centered at 512 nm (2.42 eV), and the emission intensity for the glass, which is annealed at 450 °C, is less intense with a redshift to 558 nm (2.21 eV). The higher temperature annealed glasses (500 and 550 °C) show no fluorescence like the unprocessed glass. The fluorescence peak and FWHM along with the cluster size are presented in Table I. A similar kind of work was reported by Gangopadhyay *et al.*,²⁰ who found fluorescence from Ag

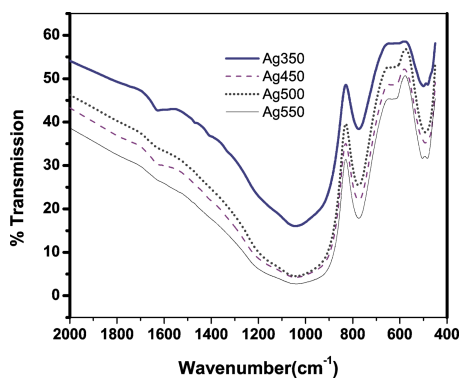


FIG. 3. (Color online) FTIR spectra for all the ion-exchanged and annealed glasses.

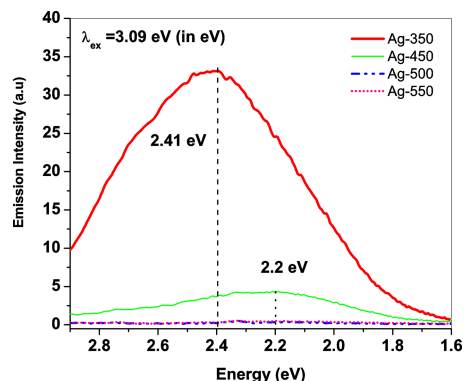


FIG. 4. (Color online) Emission spectra of the Ag nanocomposite glasses annealed at different temperatures.

nanocomposite glasses, but the fluorescence intensity increases with annealing temperature and then reduces. He attributed that the fluorescence is from excitonic photoemissions in AgO. Another work by Manikandan *et al.*²³ attributed that the fluorescence from silver clusters is due to $4d^{10}5s \leftarrow 4d^{10}5p$ transitions of (Ag^{2+}) pairs, which are the nucleation centers in the precipitation of the Ag nanoclusters inside the glass. Their study shows that when the annealing temperature increases, the emission intensity also increases but for higher annealing temperature, the glasses show no emission. In both cases, the annealing temperatures almost agree with the present case. However, in the present case, there is an intense fluorescence from the 350 °C annealed glasses; the fluorescence intensity decreased and became zero for higher temperature annealed glasses.

Fluorescence from the thin metal surfaces of Au and Cu is explained by Mooradian,²⁴ which is due to the radiative recombination of the electrons in the s - p conduction band near the Fermi surface and the holes in the d bands generated by optical excitation.

Based on the above discussion, we assign the fluorescence from the Ag-350 glass to the combination of excitonic photoemissions in AgO, and the radiative recombination of the electrons in the s - p conduction band near the Fermi surface and the holes in the d band generated by optical excitation in Ag intermediate clusters (moleculelike clusters). When the annealing temperature increases, the cluster size increases, which will reduce the energy gap between the s - p band and d band. This may be the reason that at 450 °C, annealed glasses (Ag-450) show lower energy fluorescence

TABLE I. Diameter of the prepared clusters and their fluorescence intensity maxima.

Sample code	Diameter of clusters through LFRS ^a (nm)	Diameter of clusters through optical absorption (nm)	Fluorescence peak maximum (eV)	FWHM (nm)
Ag-350	2	...	2.41	169
Ag-450	2.1	2	2.2	198
Ag-500	3	2.7
Ag-550	3.1	3.3

^aReference 18.

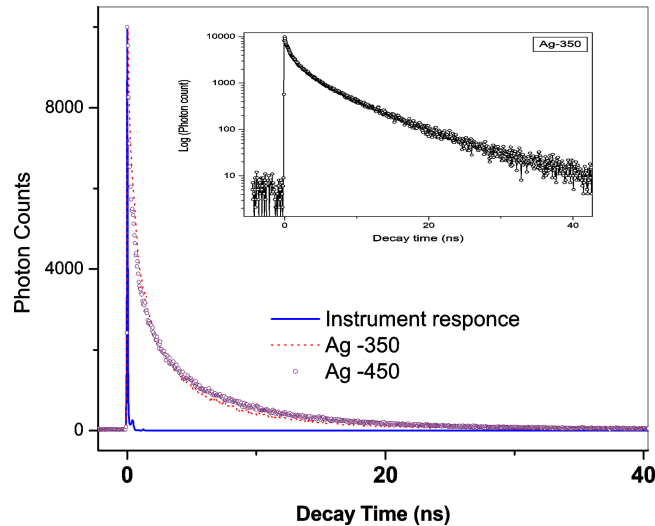


FIG. 5. (Color online) Time resolved photoluminescence measurements of Ag-350 and Ag-450 glasses, where the excitation is at 400 nm and the photon counting was done at 540 nm.

peak than 350 °C annealed glasses, which is indicated in the fluorescence spectra by the redshift. This above results can be explained by Kubo's model.

According to Kubo's model, the mean level spacing $\delta(E_F)$ near the Fermi level is given by²⁵

$$\delta(E_F) = \frac{3}{2} \frac{E_F}{N_A Z} > K_B T, \quad (5)$$

where N_A is the number of atoms in the cluster, Z is the valence of the atom, and E_F is the Fermi energy of the metal. Thus, when the number of atoms in the cluster increases, the mean level spacing decreases ($\delta(E_F) \ll K_B T$), which favors a nonradiative decay. Hence, for bigger clusters, the de-excitations become mostly nonradiative, while for intermediate and smaller clusters, radiative emission becomes more probable.

Nanoclusters in this type of glasses show very less polydispersity¹² (see Fig. 2), so the mean radii of the clusters are considered for the above discussion. This type of glasses comes under the Maxwell–Garnett effective medium approach, where the nanoclusters were dispersed in the matrix randomly and uniformly. Moreover, the mean level spacing of the clusters is higher than the diameter of the clusters. So, the interactions between the clusters are excluded in the present study.

Figure 5 shows the time resolved fluorescence at 530 nm (2.334 eV) from the Ag-350 and Ag-450 glasses with excitation at 400 (3.06 eV) nm. At this excitation wavelength, the photon energy is near the silver's SPR regime. One observes a sharp rise in the time resolved fluorescence, followed by a fast decay and a long lived component. In metal clusters, excited state electrons will decay through electron-electron ($e-e$), electron-phonon ($e-ph$), and phonon-phonon ($ph-ph$) scattering, and through radiative recombination.²⁶ Usually, the $e-e$, $e-ph$, and $ph-ph$ will be much faster than radiative recombination and will be over in the order of a few picoseconds. In our previous study,²⁷ degenerate pump probe measurements at 400 nm (100 fs pulses) on Ag-550 show

TABLE II. Exponential fit parameters of time resolved photoluminescence.

Sample name	A_1	A_2	A_3	t_1 (s)	t_2 (s)	t_3 (s)
Ag-350	8.95	29.96	61.09	2.51×10^{-10}	1.56×10^{-9}	6.22×10^{-9}
Ag-450	7.29	20.77	71.94	1.77×10^{-10}	1.40×10^{-9}	6.78×10^{-9}

that the complete recovery happened within 10 ps. In the present case, it is clear that the long lived component exists up to 40 ns. This shows that the excitation at 400 nm (3.06 eV) leads to the excitation of valence band (d band) electrons into the conduction band (sp band) through interband transitions, and radiative recombination is followed by an initial electronic scattering process giving rise to the visible luminescence. Similar kind of long lived decay dynamics was reported in Au8 clusters.²⁸ The decay fits well with the three exponential decay equation $y = A_1 \exp(t/t_1) + A_2 \exp(t/t_2) + A_3 \exp(t/t_3)$. The fitted values are presented in Table II. Interestingly, both the glasses show almost same decay times.

IV. CONCLUSION

In summary, silver nanocomposite glasses were prepared through ion-exchange method. Thermal annealing induces size growth in the clusters. The optical absorption measurements show the presence of Ag clusters and its size growth with annealing temperature. Size determination of Ag clusters using optical spectroscopy agrees well with the low frequency Raman spectral studies. Fluorescence measurements show that smaller clusters exhibit a broad fluorescence, which is due to interband transition.

ACKNOWLEDGMENTS

The author wishes to thank Reji Philip and A. K. Sood for their continuous encouragement to finish this work. The author also thanks India's National Nanoscience Initiative facility in Indian Institute of Science (IISc, Bangalore), where the TEM image was recorded, and the National Center for Ultrafast Process (NCUFP-Chennai) for their help to record the time resolved photoluminescence measurements.

¹R. H. Magruder III, D. H. Osborne, Jr., and R. A. Zuhr, *J. Non-Cryst. Solids* **176**, 299 (1994); X. Jiang, J. Qiu, H. Zeng, C. Zhu, and K. Hirao, *Chem. Phys. Lett.* **391**, 91 (2004).

²S. Qu, C. Zhao, X. Jiang, G. Fang, Y. Gao, H. Zeng, Y. Song, J. Qiu, C. Zhu, and K. Hirao, *Chem. Phys. Lett.* **368**, 352 (2003).

³I. Belharouak, F. Weill, C. Parent, G. L. Flem, and B. Moine, *J. Non-Cryst. Solids* **293–295**, 649 (2001).

⁴G. Mie, *Ann. Phys.* **25**, 377 (1908).

⁵O. Varnavski, R. G. Ispasoiu, L. Balogh, D. Tomalia, and T. Goodson III, *J. Chem. Phys.* **114**, 1962 (2001).

⁶J. Zheng, C. Zhang, and R. M. Dickson, *Phys. Rev. Lett.* **93**, 077402 (2004).

⁷M. A. Noginov, G. Zhu, M. Bahoura, C. E. Small, C. Davison, and J. Adegoke, *Phys. Rev. B* **74**, 184203 (2006).

⁸H. Mertens and A. Polman, *Appl. Phys. Lett.* **89**, 211107 (2006).

⁹L. A. Peyser, A. E. Vinson, P. A. P. Bartko, and R. M. Dickson, *Science* **291**, 103 (2001).

¹⁰S. Link, A. Beeby, S. FitzGerald, M. A. El-Sayed, T. G. Schaaff, and R. L. Whetten, *J. Phys. Chem. B* **106**, 3410 (2002).

¹¹S. Bera, P. Gangopadhyay, K. G. M. Nair, B. K. Panigrahi, and S. V. Narasimhan, *J. Electron Spectrosc. Relat. Phenom.* **152**, 91 (2006).

- ¹²M. Dubiel, H. Hofmeister, G. L. Tan, K. D. Schicke, and E. Wendler, *Eur. Phys. J. D* **24**, 361 (2003).
- ¹³U. Kreibig, G. Bour, A. Hilger, and M. Gartz, *Phys. Status Solidi A* **175**, 351 (1999).
- ¹⁴H. Hovel, S. Fritz, U. Kreibig, and M. Vollmer, *Phys. Rev. B* **48**, 18178 (1993).
- ¹⁵B. N. J. Persson, *Surf. Sci.* **281**, 153 (1993).
- ¹⁶P. V. Kamat, *J. Phys. Chem. B* **106**, 7729 (2002).
- ¹⁷P. Gangopadhyay, R. Kesavamoorthy, K. G. M. Nair, and R. Dhandapani, *J. Appl. Phys.* **88**, 4975 (2000).
- ¹⁸B. Karthikeyan, J. Thomas, and R. Kesavamoorthy, *J. Non-Cryst. Solids* **353**, 1346 (2007).
- ¹⁹P. Gangopadhyay, P. Magudapathy, R. Kesavamoorthy, B. K. Panigrahi, K. G. M. Nair, and P. V. Satyam, *Chem. Phys. Lett.* **388**, 416 (2004).
- ²⁰P. Gangopadhyay, R. Kesavamoorthy, S. Bera, P. Magudapathy, K. G. M. Nair, B. K. Panigrahi, and S. V. Narasimham, *Phys. Rev. Lett.* **94**, 047403 (2005).
- ²¹P. Gangopadhyay, R. Kesavamoorthy, K. G. M. Nair, and R. Dhandapani, *J. Appl. Phys.* **88**, 4975 (2000).
- ²²T. G. Kim, Y. W. Kim, J. S. Kim, and B. Park, *J. Mater. Res.* **19**, 1400 (2004); M. Dubiel, S. Brunsch, U. Kolb, D. Gutwerk, and H. Bertagnolli, *J. Non-Cryst. Solids* **220**, 30 (1997).
- ²³D. Manikandan, S. Mohan, and K. G. M. Nair, *Mater. Res. Bull.* **38**, 1545 (2003).
- ²⁴A. Mooradian, *Phys. Rev. Lett.* **22**, 185 (1969).
- ²⁵T. G. Schaaff, M. N. Shafigullin, J. T. Khoury, I. Vezmar, R. L. Whetten, W. G. Cullen, P. N. First, C. Gutierrez-Wing, J. Ascensio, and M. J. Jose-Yacaman, *J. Phys. Chem. B* **101**, 7885 (1997).
- ²⁶M. Adelt, S. Nepijko, W. Drachsel, and H.-J. Freund, *Chem. Phys. Lett.* **291**, 425 (1998).
- ²⁷B. Karthikeyan, J. Thomas, and R. Philip, *Chem. Phys. Lett.* **414**, 346 (2005).
- ²⁸J. Zheng, J. T. Petty, and R. M. Dickson, *J. Am. Chem. Soc.* **125**, 7780 (2003).